

The Geochemical Features of Microbial Carbonates of the Abalak and Georgian Formations in Western Siberia

M. R. Latypova^a, * (ORCID: 0000-0001-8258-9012), A. G. Kalmykov^a, ** (ORCID: 0000-0002-8862-8227),
V. V. Churkina^a, *** (ORCID: 0000-0001-7466-1598), E. V. Karpova^a, **** (ORCID: 0000-0003-3094-2253),
N. S. Balushkina^a, ***** (ORCID: 0000-0001-5900-2041),
and G. A. Kalmykov^a, ***** (ORCID: 0000-0001-8274-3622)

^a Moscow State University, Moscow, 119991 Russia

*e-mail: margarita.r.latypova@gmail.com

**e-mail: a.g.kalmykov@gmail.com

***e-mail: Lera.keily@gmail.com

****e-mail: karpoff_2002@mail.ru

*****e-mail: nataliabalushkina@mail.ru

*****e-mail: gera64@mail.ru

Received September 27, 2022; revised November 2, 2022; accepted August 16, 2023

Abstract—The geochemical and lithological features of bacterial–algal structures from the top of the Abalak and Georgia Formations in the central part of Western Siberia were studied in order to determine the specific conditions of their formation. The authors compared the element composition of these microbial carbonates with the secondary carbonate rocks of the Abalak and Georgia formations. According to the results of X-ray fluorescence analysis, differences were identified in the contents of MnO, Cr, V, Ni, Cu, and Zn in two types of carbonates. The higher content of MnO in bacterial–algal structures were explained by the ability of bacteria to sorb Mn on the surface of their cells. This process requires oxygen, which suggests the presence of a natural aerobic environment for the development of bacteria during the period of sediment accumulation. According to the results of the study of microbial carbonates under a scanning electron microscope, it was revealed that Mn, for the most part, is concentrated in carbonate minerals, in particular in kutnohorite. The increased content of biophilic elements such as Ni, Cu, Zn, V in microbial carbonates, is probably associated with the transformation of humic organic matter, that was accumulated in shallow water environments and was actively recycled by microbial organisms. Minerals with the high Ba concentration were also found in isolated bacterial–algal structures. According to the authors, such single barium mineralization could be caused by the point effect of both near-surface and deep-seated barium-containing solutions and are not associated with an increased content of manganese in the studied deposits.

Keywords: Abalak Formation, Georgia Formation, bacterial–algal structures, microbial carbonates, manganese mineralization, humus formation

DOI: 10.3103/S0145875223050071

INTRODUCTION

The study of carbonate rocks of the Abalak (J_2bt^3 – J_3tt^1) and Georgia (J_3ox^3 – J_3tt^1) formations of the West Siberian oil and gas bearing basin (WSOGB) has recently become increasingly important due to the new data on their potential reservoir properties (Zubkov, 2014; Yurchenko et al., 2015; Potapova et al., 2018). The petrophysical properties of these rocks were directly affected by their formation conditions, reflected in specific lithological and geochemical features. The stable oxygen and carbon isotope ratios in carbonates were considered most thoroughly (Yurchenko, 2016; Zubkov, 2017). There are, however, numerous traces of diagenetic and catagenetic processes that could

have strongly influenced $\delta^{13}C$ and $\delta^{18}O$, and thereby prevent identification of sedimentation settings. The trace elements in the carbonates, which, despite secondary processes, can reflect quite accurately the processes of sediment formation remain relatively less studied. We believe that the geochemical study of carbonates may add significantly to the data obtained from the complex lithological study and contribute to identification and characteristics of various aspects of carbonate formation.

The purpose of this work was to determine the specific formation conditions of bacterial–algal assemblages from the upper subformation of the Abalak Formation and from the roof of the Georgia Formation



Fig. 1. Images of bacterial–algal structures.

(Fig. 1). Obviously, formation of these sediments differed from the over- and underlying clayey and siliceous-clayey rocks, and additional data on the formation conditions of Late Jurassic microbial carbonates (MCs) of the WSOGB can significantly add to the picture of the geologic history of the region.

The Late Jurassic MCs of the WSOGB were previously studied by many researchers (Ushatinsky and Zaripov, 1971; Yasovich, 1971; Zanin et al., 2001; Eder et al., 2018). Potapova et al. (2018) described MCs from the upper Abalak Formation as fractured and cavernous rocks through which oil enters the territory

of the Em-Egovskoye field (Krasnoleninskiy arch, Western Siberia). These authors also discovered signs of subaerial exposure in carbonates from the Abalak Formation roof for the first time. The exogenous influence has probably caused extensive karstification and subsequent formation of a carbonate horizon of paleo soils in these rocks. These authors also believe that the Late Jurassic MCs acquired a complex system of secondary voids due to subaerial exposure, which resulted in improved reservoir properties.

Anomalies in mineral composition are always most clearly seen when the studied sediments are compared with typical widespread rocks. Therefore, the authors also compared MCs with secondary carbonates (SCs), the most common carbonate rocks of the Abalak and Georgia formations. This group comprised the carbonate nodules and lenses formed in the sediment during diagenetic and catagenetic secondary processes (Fig. 2a) and replacement limestones forming interlayers up to 30 cm, rarely up to 1 m in thickness (Fig. 2b). The replacement limestones were formed as a result of intensive recrystallization of primary sedimentary carbonate rocks, but rarely contain relics of primary textures, which complicates the determination of their initial genesis.

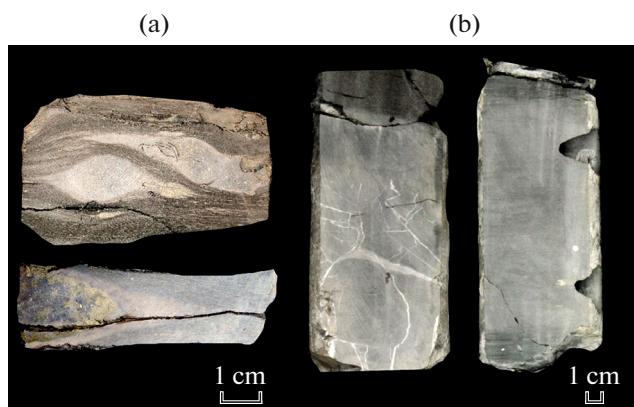


Fig. 2. Images of secondary carbonate samples: (a) carbonate diagenetic and catagenetic lenses and nodules; (b) replacement limestones, difficult to diagnose in the well core.

MATERIALS AND METHODS

The bacterial–algal structures are confined in the section to the roof deposits of the upper subformation of the Abalak Formation and the upper part of the Georgia Formation (Fig. 3a). Secondary limestones

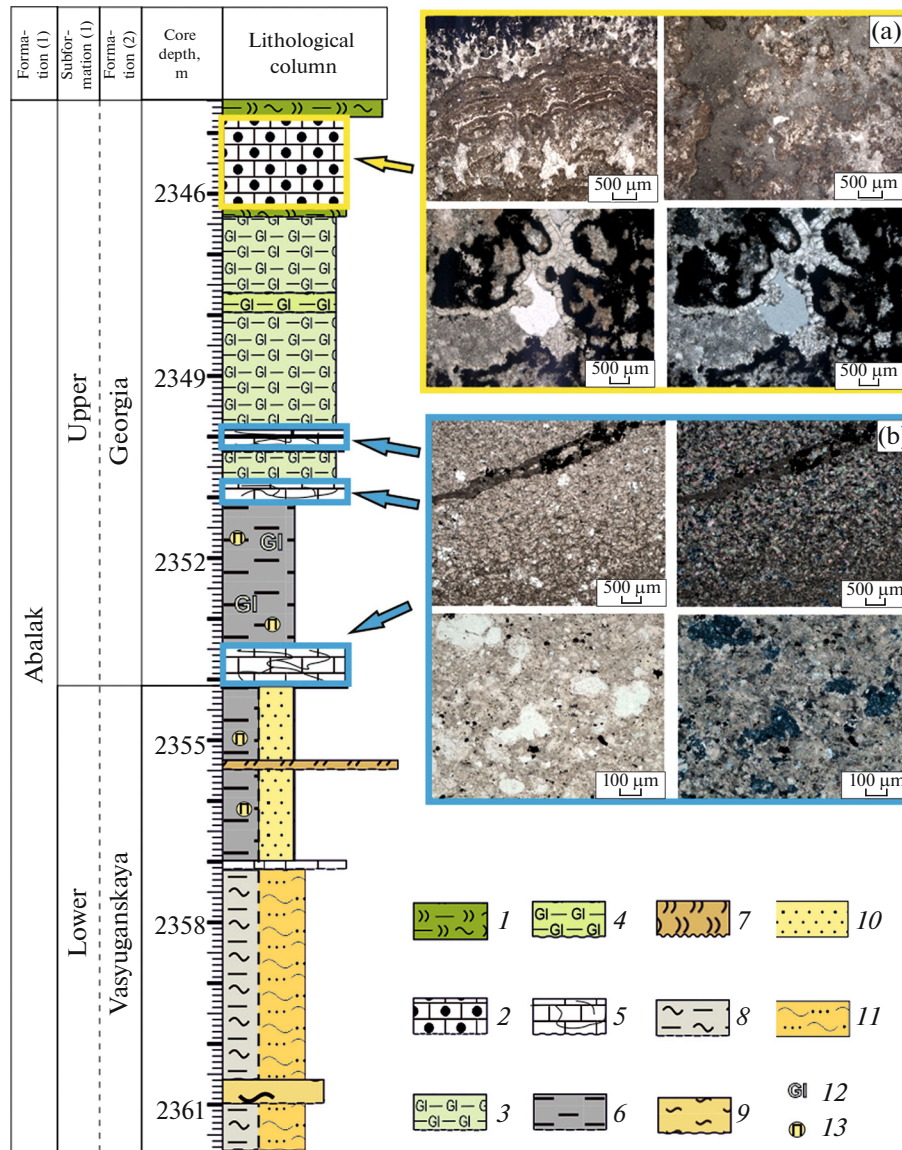


Fig. 3. A lithologic column for deposits of the Abalak, Georgia, and Vasyuganskaya formations; a, images of microbial carbonate thin sections (parallel and crossed nicols); b, images of secondary limestone slits (parallel and crossed nicols). (1) Aleurolite-clay-siliceous rocks of the Tutleim Formation; (2) bacterial-algal carbonate structures; (3) glauconite-clayey rocks; (4) clayey-glauconite rocks; (5) limestones with secondary alteration; (6) clayey rocks; (7) siliceous interlayers; (8) silty-clayey rocks; (9) siltstones; (10) sandstones; (11) sandy siltstones; (12) glauconite accumulations; (13) pyrite concretions.

are usually present in the bulk of glauconite-clayey deposits of the upper Abalak and Georgia subformations (Fig. 3b). The age and facies analogues (the upper subformation of the Abalak formation and Georgia Formation) are represented as a rule by argillite-like dark gray, thinly dispersed clays with irregularly distributed glauconite. The Vasyugan Formation, composed mainly of sandstones, sandy siltstones and mudstones, lies beneath the Georgia Formation. Its age analogue is the lower subformation of the Abalak Formation. It is composed mostly of dark argillite-like clays with pyrite concretions. The deposits of the Aba-

lak Formation are spread within the territory of the Kazym-Kondinsk and Frolovsk-Tambei facies, while the Vasyugan and Georgia formations occur within the Purpeia-Vasyugan area (*Reshenie...*, 2004).

Eleven MC and 18 SC samples of the Abalak and Georgia formations were collected from cores of the wells drilled mainly in the central part of Western Siberia. The core material revealing sedimentary cover deposits was collected from the following structural uplifts: (1) Em-Egovskaya; (2) Yuzhno-Yagunskaya; (3) Druzhnaya; (4) Lontyn-Yakhskaya; (5) Talinskaya; (6) Malobalykskaya (Fig. 4).

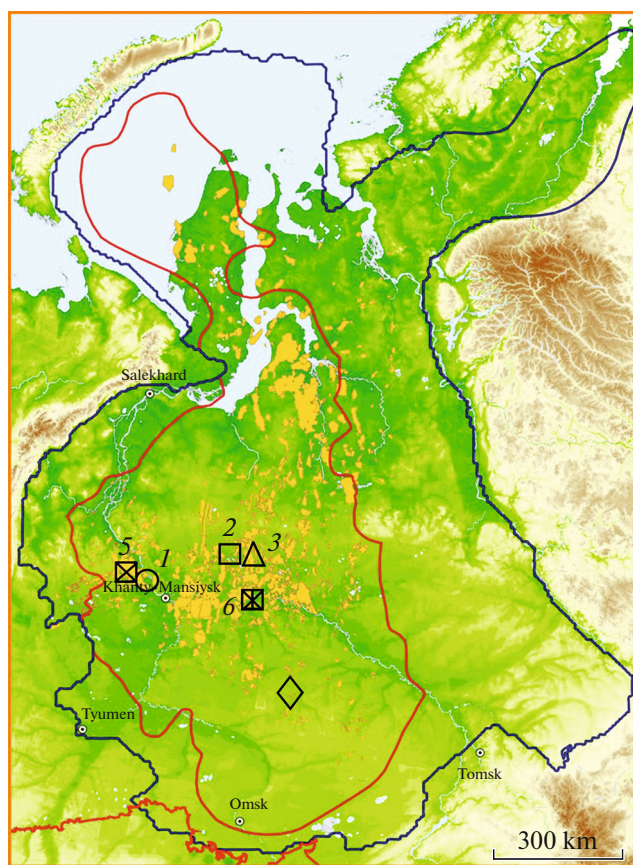


Fig. 4. A fragment of the actual map of the WSOGB (figures and symbols stand for the wells); black contour, boundaries of the West Siberian oil and gas province, red contour, boundaries of the Bazhenov complex; yellow zones mark the main hydrocarbon reserves.

The analysis of major oxides and trace elements in samples from the two types of carbonates was performed by X-ray fluorescence spectrometry (XRF) according to the analytical procedure certified by the Scientific Council on Analytical Methods of the All-Russian Research Institute of Mineral Raw Materials (NSAM VIMS), (analyst A. Yakushev) (*Metodika...*, 2000). Analysis, (excitation and registration of the characteristic radiation intensity of the elements to be determined) was performed with sequential Axios mAX Advanced X-ray fluorescence spectrometer with wavelength dispersion, manufactured by PANalytical. Samples were ground on a jaw crusher and vibration mill to a size of <0.074 mm without preliminary drying and prepared for spectrometer measurements. Glassy disks were made for rock-forming element analysis by melting baked sample with lithium borate at 1200°C in gold-platinum crucibles in a MiniFuse induction melting furnace (manufactured by Philips). Mounts for the trace element and sulfur analyses were made by cold pressing of dry sample powder with the addition of plastic filler (polystyrene).

The carbon and oxygen isotope compositions were measured using DeltaV Advantage isotope mass spectrometer (Germany) in order to determine the genetic type of carbonate rocks and find traces of secondary high-temperature processes. Samples of the two carbonate types were treated with polyphosphoric acid on a GasBenchII sample preparation line connected directly to the mass spectrometer. The composition of stable isotopes of carbon ($\delta^{13}\text{C}$) and oxygen ($\delta^{18}\text{O}$) of carbon dioxide released from the reaction of carbonates with acid was analyzed. The accuracy of the measurements was controlled with the NBS-18 and NBS-19 international standards. Isotope values are given in ‰ relative to VPDB.

The lithologic composition of both rocks types was determined from 0.02 mm-thick rock sections mounted on epoxy resin. Description and photographing of the thin sections was performed using an Olympus microscope purchased under the MSU development program.

A more detailed study of mineral composition was carried out under the scanning electron microscope (SEM) JSM-6480LV (Jeol, Japan) at the Institute of Geography of the Russian Academy of Sciences. SEM images were taken from the chips of microbial carbonate samples with high Mn content. The sample prepared for the SEM imaging had a 1–2 μm -thick gold layer sputtered on the surface with HeliosNanolab 600 unit. SEM images were processed using DigitalMicrograph and TIA software (United States).

RESULTS AND DISCUSSION

The lithologic composition of the thin sections. Lithologic description of the thin carbonate rock sections revealed that the sediments from the roof of the Abalakand Georgia formations, described as MCs, are represented by dolomitic limestones with microbial algal and secondary spherulitic structures (Fig. 5). These rocks are composed of a clotted and lumpy microbial mass with stromatolitic and disordered textures. This mass is probably the result of algal and bacterial activity.

There was, as a rule, no free pore space in the MC samples we studied; however, roughly unidirectional (along the layers of bacterial–algal structure) up to 1 mm-wide cracks filled with calcite and dolomite spheroid aggregates were quite common (Figs. 5a, 5b, 5d–5e). There were also areas filled with micro- to coarse-crystalline dolomite. Clay-phosphate material (15%) is concentrated in the form of layers and lenses with indistinct boundaries, which envelope form textural stromatolite elements. Numerous secondary, probably diagenetic and catagenetic alterations such as intense secondary dolomitization, section silicification ($<3\%$) and pyriteization (about 10%) are also noteworthy. Pyrite forms irregularly scattered aggregates of irregular and spherical shapes, up to 0.9 mm in

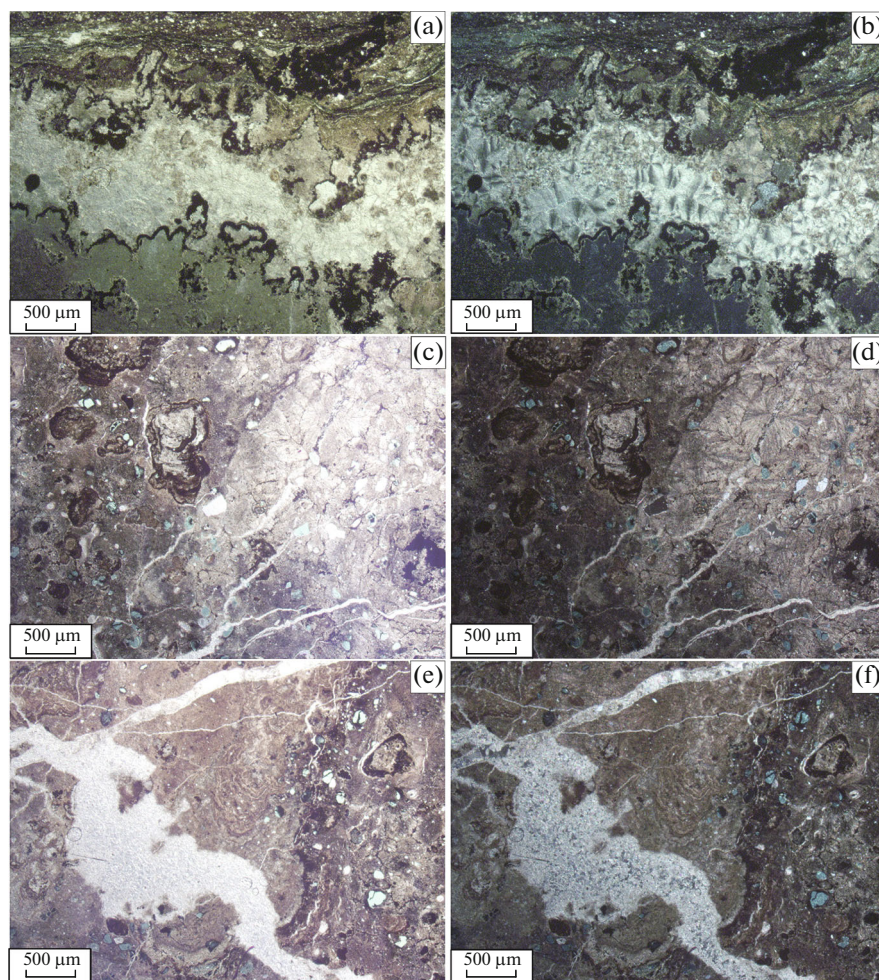


Fig. 5. Images of thin sections of microbial dolomitic carbonates; (a, c, e) parallel nicols; (b, d, f) crossed nicols.

size. The crystalloclasts include glauconite fragments (up to 10–15%) with signs of redeposition and sub-rounded silty quartz grains (up to 5%) (Figs. 5c–5d).

SCs observed in the thin rock sections are represented by massive limestones with crystalline and spheroid aggregates. Stylolite seams, formed as a result of dissolution of carbonate matter (Figs. 6a–6d), are also frequently traced in the thin sections. Angular clasts of quartz and feldspar up to 0.05–0.06 mm in diameter, as well as mica (muscovite) fragments up to 0.05 mm in size are often traced in the main mass of micrite, partially recrystallized during secondary alteration. Authigenic albite, glauconite, dolomite, crystalline and spheroaggregate calcite, micrograined siderite, as well as pyrite and chlorite, are also distinguished in the thin sections. Organic matter is distributed irregularly and often found in the form of thin films and concretions and sometimes fills small stylolitic seams. In general, no relic primary structures are observed in the secondary carbonates, which makes it impossible to determine their primary genesis.

The contents of major oxides obtained by the XRF method. The percentages of petrogenic oxides in SCs and MCs were obtained from trace element compositions obtained by the X-ray fluorescence method.

MCs differ from SCs, as a rule, by a large amount of MnO (Fig. 7a). The content of this oxide in bacterial–algal structures varies from 3 to 19%, while in SCs it ranges from 0 to 1%. This difference can probably be explained by the fact that Mn^{2+} is adsorbed on the surface of bacterial cells, which are actively involved in the formation of bacterial–algal limestones. Bacteria often act as an inhibitor of divalent Mn oxidation, as there are species that derive energy from its oxidation (Emerson et al., 1979, Yakushev et al., 2009). At the same time, manganese oxides, as a rule, actively participate in humus formation and firmly retain such heavy metals as Co, Ni, Zn, etc. in their lattice (Manceau et al., 2000).

Secondary diagenetic manganese mineralization was also explained by the concept of cyclic bacterial activity, comprising two cycles, namely, bottom aerobic chemo- lithoautotrophic cycle and anaerobic dia-

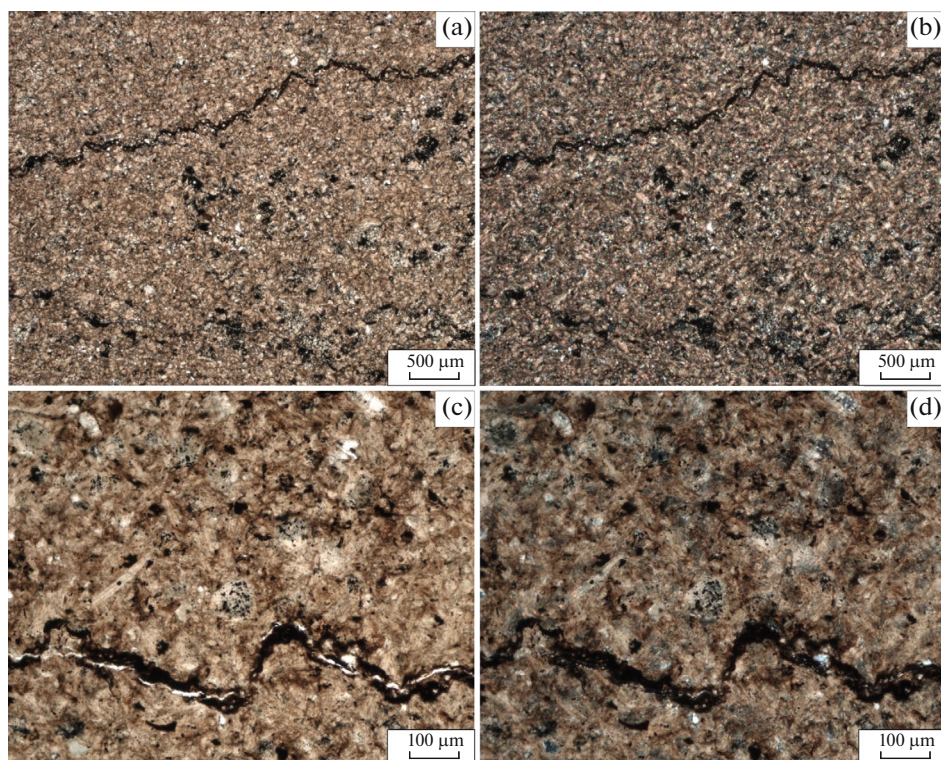


Fig. 6. Images of thin sections of secondary carbonates (a, c) parallel nicols; (b, d) crossed nicols.

genetic bacterial cycle, with the anaerobic system overlapping the aerobic one (Polgari et al., 2012). The oxidation of Mn(II) to Mn(III, IV) due to bacterial activity, as well as the release and sorption of metal ions on the MnO surface during the decomposition of organic molecules occur within the benthic aerobic oxidative cycle. Later, the bottom oxygen environment is overlapped by a series of sediments, which leads to a change to an oxygen-free reducing (anaerobic-sub-oxic) environment. Microbiologically mediated reduction of Mn(III, IV), occurring in such an environment, leads to Mn-carbonate mineralization.

The behavior of Mn in these carbonates is still poorly studied; however, there were observations of the increased content of this element in diagenetic carbonate nodules of the Bazhenov and Tutleimskaya J₃ formations (Ushatinsky et al., 1970, Yudovich and Ketris, 1988). The even higher concentration of Mn in bacterial–algal structures of the underlying Abalak and Georgia formations can be explained by the high oxygen content in bottom waters due to shallowing of the basin. It is known that periodic aeration of deep-water depressions in the Baltic Sea during strong storms leads to the transfer of Mn into sediments (Zelenin and Ozerov, 1983). It is also likely that Mn may be more actively accumulated in MCs due to their growth in shallow well-aerated waters. In addition, stagnant conditions could also enhance Mn precipitation into the sediment, because under distinctly stag-

nant conditions of the water column, the concentrations of components are equalized, the diffusion of manganese from sediment to water slows, and Mn remains in the upper ooze film and precipitates as MnCO₃ (Blazhchishin and Emelyanov, 1977). This scenario, however, is possible only in the presence of a large amount of carbonate material in the ooze (Berger and Soutar, 1970).

The contents of other major oxides vary insignificantly within the margin of error and depend on the area. Thus, the content of MgO in MCs from the territory of Em-Yegovsky, Lontyn-Yakhsky, Talinsky and Malobalyksky uplifts (3–8%) is often higher than that in SCs (1–4%). The opposite pattern was traced for samples from the area of Druzhnaya summit. 3-MC samples generally contain less MgO (1–5%) than 3-SC ones (8–9%). Similarly, the SiO₂ content in bacterial–algal structures of the Yuzhno-Yakunskoe, Druzhnoe, and Talinskoe uplifts is, on average, higher (8–18%) than that in SCs (1–13%). There is also a slight difference in the contents of all other oxides between the two types of carbonate rocks depending on the confinement to the deposit.

The trace element composition according to XRF data. The two types of carbonate rocks differ more significantly in terms of elemental impurities (Fig. 7b). As a rule, bacterial–algal carbonates contain more Ni, Cu, Zn, V, and less Sr. The Ni content in MC is significantly higher (220–2067 ppm) than in SCs (up to

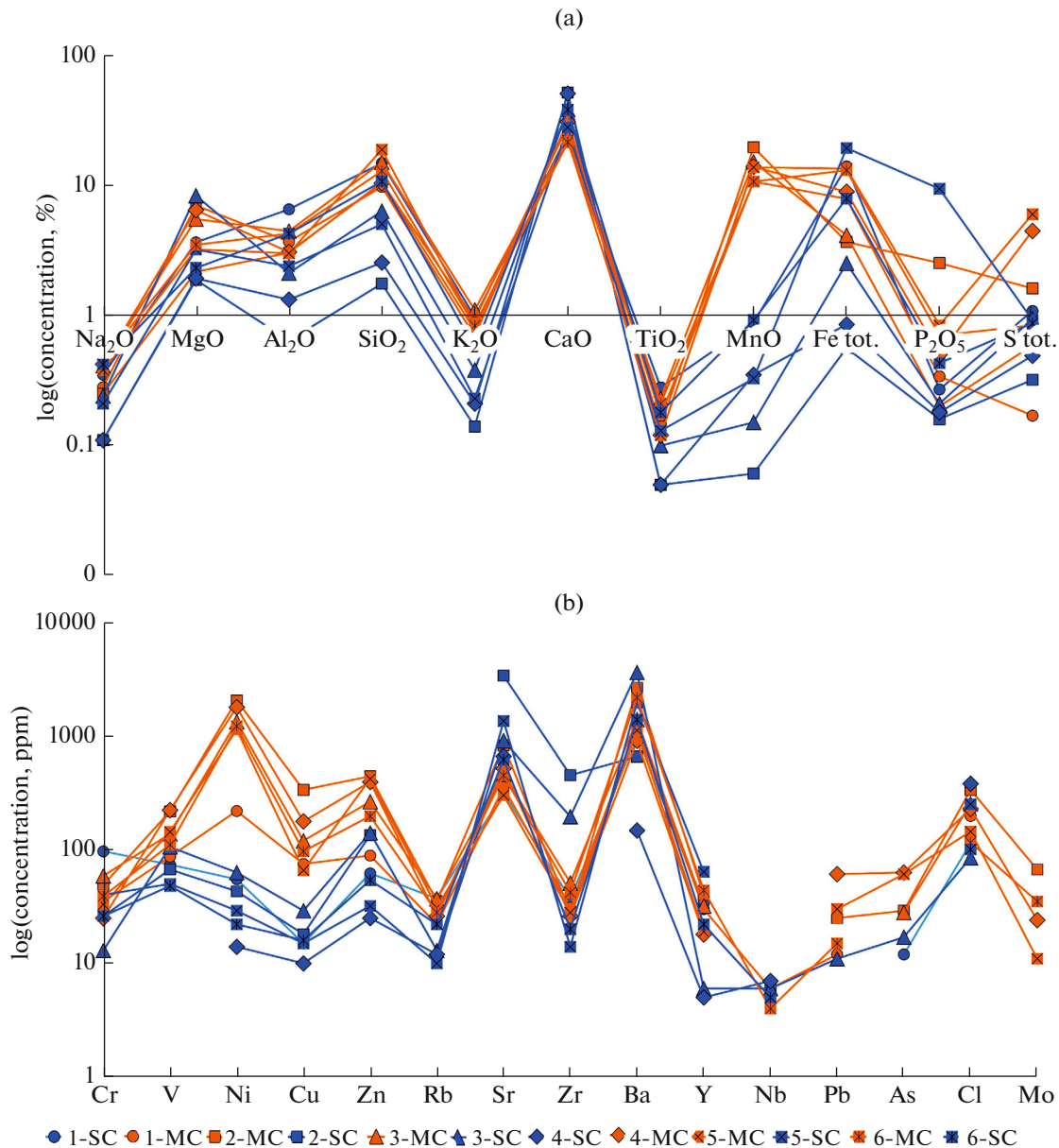


Fig. 7. A multi-element diagram with a logarithmic vertical axis for petrogenic oxides (a) and for elemental impurities (b) in carbonate rocks of the Abalakszkaya and Georgievskaya formations (yellow, MCs; blue, SCs). Samples taken from the studied uplifts: (1) Em-Egovskoye; (2) Yuzhno-Yagunskoye; (3) Druzhnoye; (4) Lontyn-Yakhskoye; (5) Talinskoye; (6) Malobalykskoe.

118 ppm) (Figs. 8a, 8b). The copper content in MCs is also significantly higher (37–338 ppm) compared to SCs (0–29 ppm) (Figs. 8a, 8c, 8d). The Zn content varies from 89 to 422 ppm, and from 25 to 215 ppm in bacterial–algal structures and SCs, respectively (Figs. 8b, 8d). In addition, there are insignificant differences in the V content for the two types of carbonates: 76–224 ppm (MCs) and 0–169 ppm (SCs) (Fig. 8e). The two types of carbonate rocks also show significant differences in Sr content: 344–833 ppm (MCs) versus 317–4833 ppm (SCs) (Fig. 8f). The contents of other trace elements in the two types of car-

bonates vary insignificantly and, similarly to most petrogenic oxides, depend rather on the territory.

The main forms of Zn transport, in our case, are probably colloids and organometallic compounds that formed under the influence of humus organic matter (Monin and Lisitsin, 1983). As mentioned above, traces of intensive karstification and a carbonate horizon of paleo-soils were previously found in the studied sediments in the territory of the Em-Egov summit (Potapova et al., 2018), which confirms this assumption. Zinc is also a biophilic element, which probably explains its higher content in bacterial–algal struc-

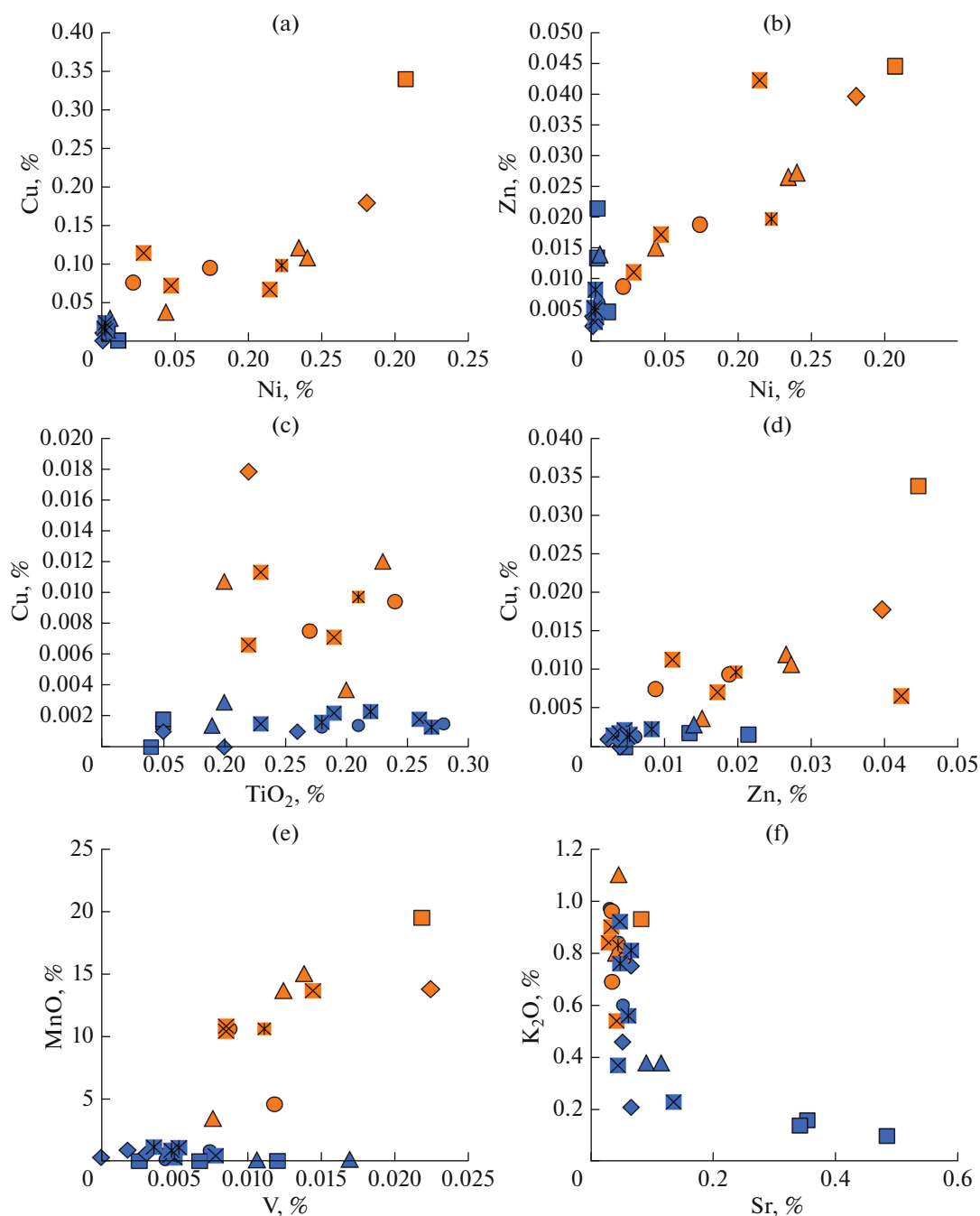


Fig. 8. Trace element ratios in carbonate rocks of the Abalak and Georgia formations (yellow, MCs; blue, SCs); samples taken from the areas studied are specified in Fig. 7.

tures compared to SCs. Considering the rhizoids (traces of roots) previously found in MCs (Potapova et al., 2019), the more intensive accumulation of biophilic elements in the surface of humus horizons of the soil layer seems logical (Mikhalechuk, 2017). Another element that gravitates to humic compounds is Ni. Some heavy metals bind with humic substances into poorly soluble colloidal film phases (Eisma, 1988; Sholkovitz, 1990). Thus, Ruban (2017), found the

maximum Ni content (410.0 ppm) in pelitic sediments of the coastal area of Buor-Khoya Bay in the eastern part of the Laptev Sea. This author associated the increased Ni content with the input of marsh humic compounds, which were activated during storms. The increased V content in bacterial–algal structures can probably also be explained by the participation of this element in the humus formation process. According to Rachold, Brumsack (2001) the concentration of V in

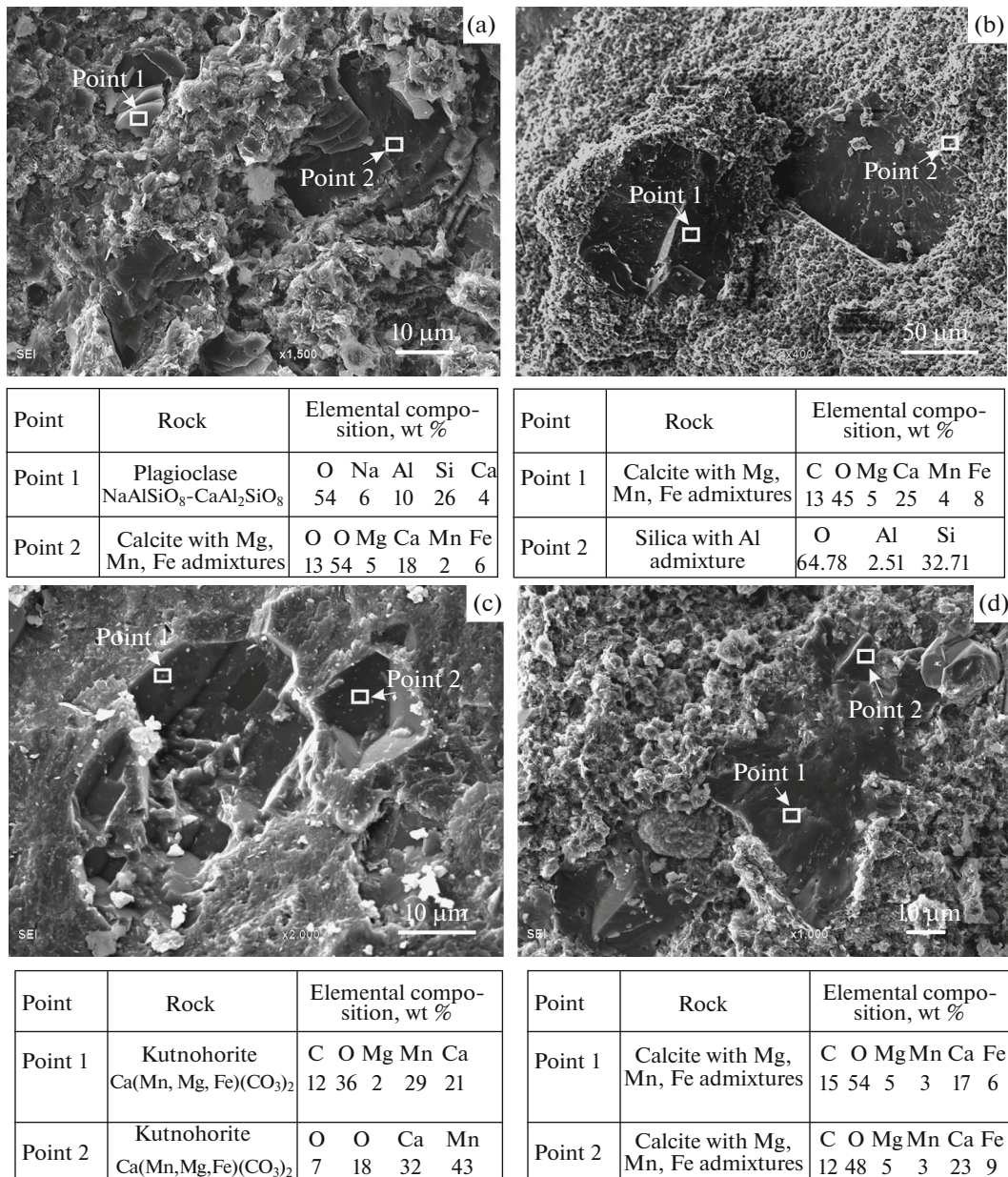


Fig. 9. SEM images and trace element composition of the MC samples.

sediments may increase under reducing conditions, as this element binds to organic matter.

The trace element composition acquired from SEM. The SEM study of MCs showed that Mn in the studied samples was concentrated mainly in carbonate minerals, namely in kutnohorite, Ca(Mn, Mg, Fe)(CO₃)₂, which composed both the main mass and separate crystals (Fig. 9c). A small amount of Mn was also observed as an admixture in calcite (Figs. 9a, 9d). All manganese carbonate minerals displayed high Ca content of 18–32 wt %, which does not allow us to draw a conclusion about the presence of pure rhodochrosite in the studied rocks. The rare single crystals of plagioclase NaAlSi₃O₈-CaAl₂SiO₈ (Fig. 9a) as well as siliceous matter with various impurities, e.g., Al, whose content does not reach 3 wt % (Fig. 9b) were found in the samples taken from bacterial–algal structures.

Various manifestations of pyrite (FeS₂), namely, isometric crystals (Figs. 10a–10c) and globules (Fig. 10d) were frequently observed in the samples. Rarely, pyrite crystals on the SEM images are covered with light precipitate with the spectra of sulfate minerals, which probably could have formed as a result of secondary sulfatization. The Ca content in these sulfates is, however, very low, up to 5 wt %, which

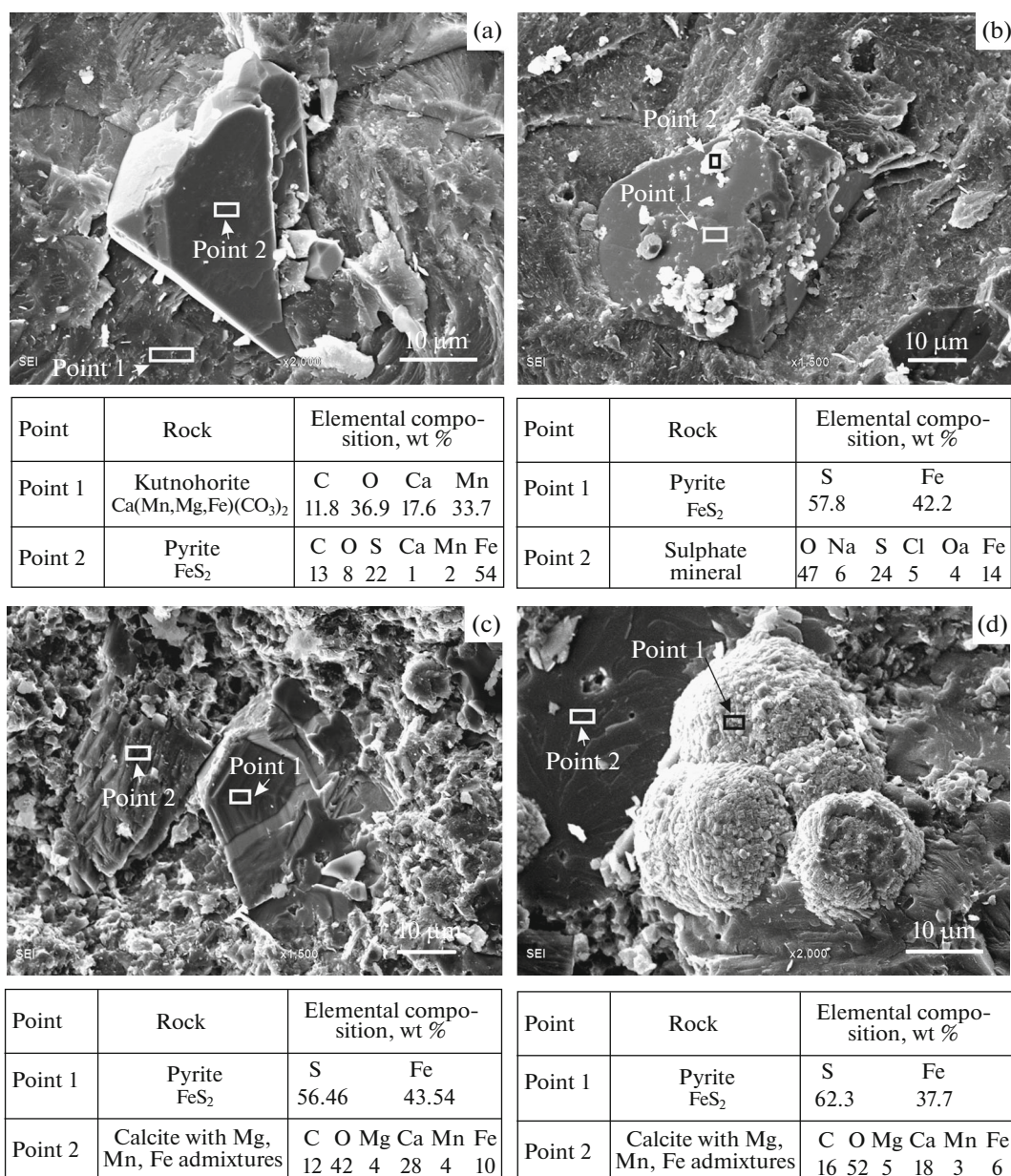


Fig. 10. SEM images and trace elemental composition of the pyrite in MCs.

excludes the presence of gypsum or anhydrite in the sediments studied (Fig. 10b).

As well, SEM images of the main carbonate mass of isolated bacterial–algal structures showed cracks filled with organic matter (Fig. 11a) or calcite with Fe, Mg, Mn impurities (Fig. 11b). Such manifestations can be attributed to traces of secondary diagenetic and catagenetic processes.

Another trace of secondary alterations in the rocks is the presence of hydrous clay minerals, in particular, glauconite $((\text{K}, \text{H}_2\text{O})(\text{Fe}^{3+}, \text{Al}, \text{Fe}^{2+}, \text{Mg})_2[\text{Si}_3\text{AlO}_{10}](\text{OH})_2 \cdot n\text{H}_2\text{O})$. In Fig 11c and minerals with high (up to 34 wt %) Ba content (Fig. 11d) in the basic kutnohorite matrix are

shown. Authigenic glauconite in the studied samples often composes grains (Fig. 11c) and spherical clusters (Fig. 11d).

As for barium carbonates, according to Karpova et al. (2021), elevated barium contents in individual samples as well as crystallization of barium-bearing minerals are one of the markers of hydrothermal flow. In fact, experiments on barite crystallization have shown that crystallization of this mineral from the mixture of Na_2SO_4 and BaCl_2 solutions in carbonate rocks is possible at 150–300°C (Kunz, 2002). According to Gurvich et al. (1978), the total Ba content in carbonate and siliceous sediments is about 0.096%. This means that the barium stored during sedimenta-

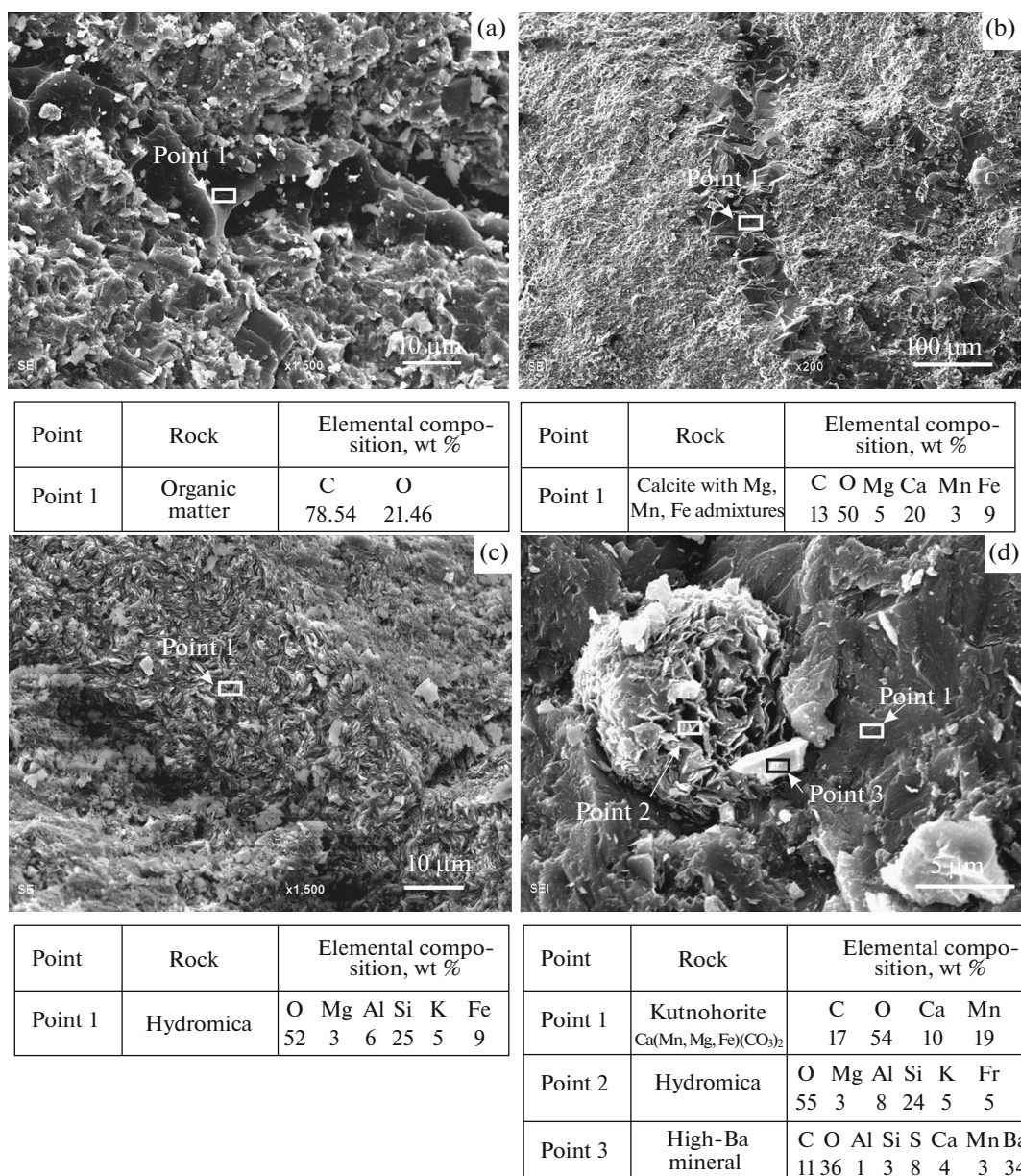


Fig. 11. SEM images and trace element composition (a) of the fracture filled with organic matter; (b) of calcite vein, (c, d) of hydrous and Ba-bearing minerals in MCs.

tion is not sufficient for the formation of Ba minerals; there should be an additional Ba source. We should not, however, attribute barium mineralization exclusively to the effect of hydrothermal fluid. The source of mobile Ba for barium-bearing fluids entering the upper horizons of sedimentary strata may be bio-barites of siliceous plankton (Von Breymann et al., 1992; Fu et al., 1994). Another mechanism that might produce barium fluids or mobilize dissolved Ba and transfer it to the upper sedimentary strata along faults, is post-sedimentary catagenetic changes of clay minerals (smectite-illite transformations) in submerging basins (Dahlmann and Lange, 2003). The mixing of cold

barium-bearing fluid flows, the sources of which are not only near-surface but also deeper reservoirs, also cannot be excluded (Derkachev et al., 2015). Since no barite (BaSO_4) was detected in the samples, there is, in the authors' opinion, no space for assumptions about the influence of SO_4 -containing acidic chloride high-temperature solutions on secondary alteration of the sediments.

Oxygen and carbon isotope composition. Isotope data obtained for the samples of two types of carbonate rocks show a significant difference in the ratios of $\delta^{18}\text{O}$ and $\delta^{13}\text{C}$ (Table 1). The $\delta^{18}\text{O}$ in SCs varies in a narrow range from -11 to -12.7‰ . Meanwhile, MCs are less

Table 1. Oxygen and carbon stable isotopes in the samples of microbial and altered secondary carbonates

Sample*	$\delta^{13}\text{C}/^{12}\text{C}$ (‰ PDB)	$\delta^{18}\text{O}/^{16}\text{O}$ (‰ PDB)
VC	-14.83	-11.01
VC	-16.80	-12.75
VC	-17.51	-12.60
VC	-16.06	-12.69
MC	-3.00	-8.74
MC	-6.22	-7.37
MC	-2.38	-7.48
MC	-3.12	-7.37
MC	-4.60	-8.31

* MCs, microbial carbonates; SCs, secondary carbonates.

enriched in light oxygen isotopes, with $\delta^{18}\text{O}$ values ranging from -7 to -8.7 ‰. The difference between the two rock types are even more pronounced in the ratio of stable carbon isotopes. $\delta^{13}\text{C}$ in SCs varied from -14.8 to -17.5 ‰. At the same time, MCs have a

heavier isotope composition, with the value of the $\delta^{13}\text{C}$ varying from -2 to -6 ‰. Such a distribution of $\delta^{13}\text{C}$ could only be caused by the degree of participation of carbon dioxide of microbial origin formed inside the sediment during oxidation of organic matter under diagenesis conditions in the process of MC formation (Kuleshov, 2013).

Thus, it can be concluded that the isotope data we obtained, namely, the relatively heavier isotope composition $\delta^{18}\text{O}$ in MCs, do not indicate high temperatures of transformation of bacterial–algal assemblages characteristic of hydrothermally transformed sediments. According to (Yurchenko et al., 2015), carbonates of the Abalak Formation of the WSOGB that were formed at elevated temperatures, in particular the group of hydrothermal carbonates, are enriched in light oxygen isotopes ($\delta^{18}\text{O}$ varies from -24 to -15 ‰ VPDB) (Fig. 12). The second group of carbonate rocks (limestones of the seep carbonate matrix), also described in (Yurchenko et al., 2015) is more enriched in light carbon isotope ($\delta^{13}\text{C}$ varies from -13.8 to -27.4 ‰ VPDB), indicating a biogenic source of car-

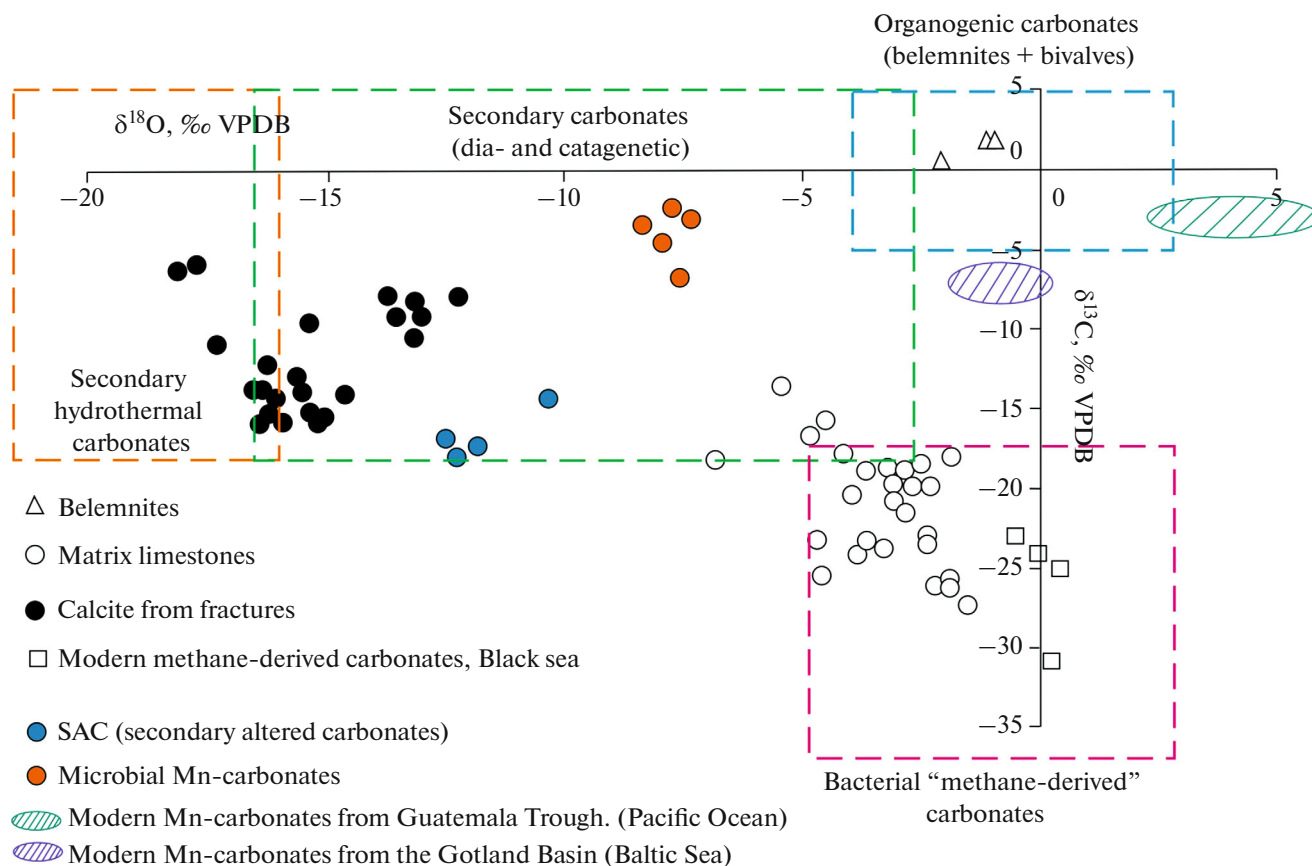


Fig. 12. The oxygen and carbon stable isotope compositions for belemnites, matrix limestones, and calcite from fractures of the Abalak Formation (Yurchenko et al., 2015), modern methane-derived Black Sea carbonates (Reitner et al., 2005), modern manganese carbonates from the Guatemalan Basin, Pacific Ocean (Coleman et al., 1982), modern manganese carbonates from the Gotland Basin, Baltic Sea (Leina et al., 1986); zones of carbonate rocks were distinguished according to (Faure, 1989; Lein et al., 2001; Campbell et al., 2002; Hinrichus and Boetius, 2002; Zakharov et al., 2006).

bon dioxide involved in their formation. Seep carbonate rocks also have a microbial genesis, but their formation took place in significantly deeper water in areas of bottom-depositing seep. The MCs studied contain heavier oxygen isotope composition than secondary hydrothermal carbonates and heavier carbon than bacterial methane-derived seep carbonates (Fig. 12). It can be inferred therefore that the studied MCs were formed at lower temperatures and under greater exposure to organic carbon dioxide.

Comparison of the isotope data for MCs of the Abalak and Georgia formations with those available for Mn carbonates from modern marine and oceanic sediments of the Pacific Ocean and the Baltic Sea shows that they are very similar in $\delta^{13}\text{C}$, indicating approximately the same contribution of organic carbon dioxide during rock formation. However, there is a significant difference in $\delta^{18}\text{O}$: Mn carbonates of modern sediments are more enriched in heavy oxygen isotope ($\delta^{18}\text{O}$ ranges from -3 to -6% VPDB). The difference in $\delta^{18}\text{O}$ can be explained by intensive secondary catagenetic transformations of the Abalak and Georgia MCs compared to the modern unaltered sediments, which is also confirmed by the SEM studies of the rocks.

CONCLUSIONS

The study revealed some peculiarities of MC genesis in the upper subformations of the Abalak Formation and in the Georgievskaya Formation of the WSOGB. The MC formation involved bacteria that probably adsorbed Mn on the surface of their cells and the subsequent manganese mineralization occurred as a result of alternation of bottom aerobic and diagenetic anaerobic cycles. Such a cyclic system required an oxygen environment in which bacteria could reproduce and cover the sediment layer by layer, creating an anaerobic diagenetic environment in which, in fact, the process of manganese mineralization took place. Thus, the presence of bacterial–algal structures in the studied section can be considered as an important indicator of good aeration of the aquatic environment in the sedimentation basin.

The high content of a whole group of biophilic elements (Zn, Ni, Cu, and V) in bacterial–algal structures compared to secondary carbonates indicates the presence of humus material in the sediment. These trace elements were probably actively involved in biogeochemical processes; the previously discovered traces of karstification and rhizoids in the MCs of the Em-Egovskaya area also support the assumption of the existence of a carbonate horizon of paleo-soils.

Comparison of the carbon isotope composition of the two carbonate types shows a large difference in $\delta^{13}\text{C}$. The heavier isotope composition of carbon in bacterial–algal structures indicates a biogenic source of carbon dioxide involved in their formation. The

similarity of the carbon isotope composition of modern microbial manganese carbonates with the studied Late Jurassic bacterial–algal structures of the WSOGB also suggests the primary biogenic nature of the latter.

SEM study of the MCs revealed that Mn is contained mainly in the kutnohorite mineral. In addition, Ba-rich minerals found in some bacterial–algal structures suggest the introduction of barium-bearing fluids. The question of the temperature and depth of these fluids, however, remains controversial because of the relatively heavy oxygen isotope composition in carbonates and the absence of the high-temperature barite mineral.

FUNDING

This work was supported by ongoing institutional funding. No additional grants to carry out or direct this particular research were obtained.

CONFLICT OF INTEREST

The authors declare that they have no conflicts of interest.

REFERENCES

- Berger, W.Y. and Soutar, A., Preservation of plankton shells in an anaerobic basin off California, *Geol. Soc. Am. Bull.*, 1970, vol. 81, no. 1, pp. 275–282.
- Blazhchishin, A.I. and Emel'yanov, E.M., Principal Features of Geochemistry of the Baltic Sea, in *Geokhimičeskije issledovaniya i poiski poleznykh iskopaemykh v Belorussii i Pribaltike* (Geochemical Prospecting for Mineral Resources in the Belarus and the Baltic), Minsk, 1977, pp. 60–156.
- Von Breyman, M.T., Brumsack, H.J., and Emeis, K.-C., Deposition and diagenetic behavior of barium in the Japan Sea, in *Proceedings of the Ocean Drilling Program Scientific Results. College Station, TX (Ocean Drilling Program)*, 1992, pp. 651–665.
- Campbell, K.A., Farmer, J.D., and Des Marais, D., Ancient hydrocarbon seeps from the Mesozoic convergent margin of California: Carbonate geochemistry, fluids and paleoenvironments, *Geofluids*, 2002, no. 2, pp. 63–94.
- Coleman, M., Fleet, A., and Donson, P., Preliminary studies of manganese-rich carbonate nodules from leg 68, suite 503, Eastern equatorial Pacific, in *Initial Reports of the Deep Sea Drilling Project (U.S. Govt. Printing Office)*, Prell, W.L., Gardner, J.V., , Eds., 1982, vol. 68, pp. 481–489.
- Dahlmann, A. and Lange, G.J., Fluid-sediment interactions at Eastern Mediterranean mud volcanoes: A stable isotope study from ODP Leg 160, *Earth Planet. Sci. Lett.*, 2003, vol. 212, pp. 377–391.
- Derkachev, A.N., Nikolaeva, N.A., Baranov, B.V., et al., Manifestation of carbonate–barite mineralization around methane seeps in the Sea of Okhotsk (the western slope of the Kuril Basin), *Oceanology*, 2015, vol. 55, no. 3, pp. 390–399.

- Eder, V.G., Follmi, K.B., Zanin, Yu.N., and Zamirailova, A.G., Manganese carbonates in the Upper Jurassic Georgiev Formation of the Western Siberian marine basin, *Sediment. Geol.*, 2017, vol. 363, pp. 221–234.
- Eisma, D., Transport and deposition of suspended matter in estuaries and the Wearsbore sea, in *Physical and Chemical Weathering in Geochemical Cycles*, Lotman, A. and Meybeck, M., Eds., 1988, pp. 273–278.
- Emerson, S., Cranston, R.E., and Liss, P.S., Redox species in a reducing fjord: Equilibrium and kinetic considerations, *Deep-Sea Res.*, 1979, vol. 26, no. 8, pp. 859–878.
- Faure, G., *Principles of Isotope Geology* (2nd ed.), Wiley, 1986.
- Fu, B., Aharon, P., Byerly, G.R., and Roberts, H.H., Barite chimneys on the Gulf of Mexico slope. Initial report on their petrography and geochemistry, *Geo-Mar. Lett.*, 1994, vol. 14, pp. 81–87.
- Gurvich, E.G., Bogdanov, Yu.A., and Lisitsyn, A.P., The barium behavior in the present-day sedimentation in the Pacific, *Geokhimiya*, 1978, no. 3, pp. 410–415.
- Hinrichus, K.-U. and Boetius, A., The anaerobic oxidation of methane: new insights in microbial ecology and biogeochemistry, in *Ocean Margin Systems*, Springer-Verlag Berlin Heidelberg, 2002, pp. 457–477.
- Karpova, E.V., Khotylev, O.V., Manuilova, E.A., et al., Hydrothermal-metasomatic systems as the most important factor for the formation of elements of the oil and gas bearing complex in the Bazhenov–Abalak sediments, *Georesursy*, 2021, vol. 23, no. 2, pp. 142–151.
- Kuleshov, V.N., *Margantsevye porody i rudy: geokhimiya izotopov, genezis, evolyutsiya rudogeneza* (Manganese Rocks and Ores: Isotope Geochemistry, Genesis, and Evolution of Ore Formation), Moscow: Geol. Inst. Ross. Akad. Nauk, Izd. Nauchn. Mir, 2013.
- Kunts, A.F., *Gidrotermal'no-metasomaticheskoe rudoobrazovanie v karbonatnykh porodakh (eksperimental'nye modeli i ikh prilozheniya)* (Hydrothermal-Metasomatic Ore Formation in Carbonate Rocks: Experimental Models and Their Implication), Yekaterinburg: Ural. Otd. Ross. Akad. Nauk, 2002.
- Lein, A.Yu., Vanshein, B.M., and Kashparova, E.V., Biogeochemistry of anaerobic diagenesis and a mass balance of sulfur and carbon isotopes in the sediments of the Baltic Sea, in *Geokhimiya osadochnogo protsesssa v Baltiiskom more* (Geochemistry of Sedimentary Process in the Baltic Sea), Moscow: Nauka, 1986, pp. 155–176.
- Lein, A.Yu., Ulyanova, N.V., and Pimenov, N.V., Black Sea “corals”—Products of mineralization of microbial mats, *Priroda (Moscow, Russ. Fed.)*, 2001, no. 12, pp. 48–54.
- Manceau, A., Lanson, B., Schlegel, M.L., et al., Quantitative Zn speciation in smelter-contaminated soils by EXAFS spectroscopy, *Am. J. Sci.*, 2000, vol. 300, pp. 289–343.
- Metodika kolichestvennogo khimicheskogo analiza. Rentgenospektral'noe fluoretsentnoe opredelenie flora, natriya, magniya, alyuminiya, kremniya, fosfora, kaliya, kal'tsiya, skandiya, vanadiya, khroma, margantsa, zheleza, kobal'ta, nikelya, strontsiya, tsirkoniya, niobiya v gornykh porodakh, rudakh i produktov ikh pererabotki. Metodika 439-RS* (Method of Quantitative Chemical Analysis no. 439-RS “Determination of Fluorine, Sodium, Magnesium, Aluminum, Silicon, Phosphorus, Potassium, Calcium, Scandium, Titanium, Vanadium, Chromium, Manganese, Iron, Cobalt, Nickel, Strontium, Zirconium, Niobium in Rocks, Ores and Their Derivatives by the X-Ray Fluorescence Method), Moscow: Vseross. Nauchno-Issled. Inst. Miner. Syr'ya, 2010.
- Mikhail'chuk, N.V., Mobile forms of heavy metals and trace elements in carbonate range soils of the southwest part of Belarus, *Proc. Natl. Acad. Sci. Belarus, Chem. Ser.*, 2017, no. 3, pp. 90–97.
- Monin, A.S. and Lisitsin, A.P., *Biogeokhimiya okeana* (Ocean Biogeochemistry), Moscow: Nauka, 1983.
- Polgari, M., Hein, J.R., Vigh, T., et al., Microbial processes and the origin of the Urkut manganese deposit, Hungary, *Ore Geol. Rev.*, 2012, vol. 47, pp. 87–109.
- Potapova, A.C., Vilesov, A.P., Chertina, K.N., et al., Signs of the subaerial exposition at the boundary between the Abalak and Tutleim (Bazhenov) formations, *Geol., Geofiz., Razrab. Neft. Gaz. Mestorozhd.*, 2018, no. 11, pp. 13–19.
- Potapova, A.C., Vilesov, A.P., Bumagina, V.A., et al., Conceptual sedimentological model of formation of carbonate rocks at the boundary between the Abalak and Bazhenov formations (Krasnoleninsk petroleum district), in *Mater. IX Vseross. litol. Soveshch. “Litologiya osadochnykh kompleksov Evrazii i shel'fovykh oblastei”* (Proc. IX All-Russ. Lithol. Conf. “Lithology of Sedimentary Complexes of Eurasia and Shelf Zones”), Kazan, 2019, pp. 367–368.
- Rachold, V. and Brumsack, H.J., Inorganic geochemistry of Albian sediments from the Lower Saxony Basin NW Germany: Palaeoenvironmental constraints and orbital cycles, *Palaeogeogr., Palaeoclimatol., Palaeoecol.*, 2001, vol. 174, pp. 121–143.
- Reitner, J., Peckmann, J., Reimer, A., et al., Methane-derived carbonate build-ups and associated microbial communities at cold seeps on the lower Crimean shelf (Black Sea), *Facies*, 2005, vol. 51, pp. 66–79.
- Reshenie 6-go mezhhvedomstvennogo stratigraficheskogo soveshchaniya po rassmotreniyu i prinyatiyu utochnennykh stratigraficheskikh skhem mezozoiskikh otlozheniya Zapadnoi Sibiri* (Resolution of the 6th Interdepartmental Stratigraphic Conference on Consideration and Approval of Improved Stratigraphic Charts for the Mesozoic Deposits of West Siberia), Novosibirsk, 2004.
- Ruban, A.S., Genetic features of modern bottom sediments of the eastern part of the Laptev Sea (on the example of Buor-Khaya Bay), *Cand. (Geol.-Mineral.) Dissertation*, Tomsk, 2017.
- Sholkovitz, E.R., Rare-earth elements in marine sediments and geochemical standards, *Chem. Geol.*, 1990, no. 88, pp. 333–347.
- Ushatinskii, I.N. and Zaripov, O.G., Mineralogy of carbonate and clay cements of productive deposits of the Shaim oil-bearing area in connection with their reservoir properties and the formation of oil fields, in *Shaimskii neftenosnyi raion. Tr. ZapsibNIGNI, vyp. 43* (Shaim Oil-Bearing Region. Trans. West Siberian Inst. Oil Gas Geol.), Nesterov, I. I., Ed., Tyumen, 1971, pp. 164–190.

- Ushatinskii, I.N., Babitsin, P.K., and Zaripova, O.G., *Metodika i rezul'taty izucheniya mineralogii glin produktivnykh otlozhenii Zapadno-Sibirskoi nizmennosti v svyazi s ikh neftegazonosnost'yu* (The Procedure and Results of Studying the Clay Mineralogy of Productive Deposits of the West Siberian Lowland in view of their Hydrocarbon Potential), Tyumen, 1970.
- Yakushev, E., Pakhomova, S., Sorenson, K., and Skei, J., Importance of the different manganese species in the formation of water column redox zones: Observations and modeling, *Mar. Chem.*, 2009, vol. 117, nos. 1–4, pp. 59–70.
- Yasovich, G.S., The formation conditions of Jurassic deposits of the Shaim and Krasnoleninsk oil-bearing areas, in *Shaimskii neftenosnyi raion, Tr. ZapsibNIGNI, vyp. 43* (Shaim Oil-Bearing Region. Trans. West Siberian Inst. Oil Gas Geol.), Nesterov, I. I., Ed., Tyumen, 1971, pp. 207–255.
- Yudovich, Ya.E. and Ketris, M.P., *Geokhimiya chernykh slantsev* (Geochemistry of Black Shales), Leningrad: Nauka, 1988.
- Yurchenko, A.Yu., Formation of secondary carbonate rocks of the Upper Abalak–Bazhenov stratum of the Salym, Pravdinsk and Malobalyk oil fields of Western Siberia, *Cand. (Geol.-Mineral.) Dissertation*, Moscow, 2016.
- Yurchenko, A.Yu., Balushkina, N.S., Kalmykov, G.A., et al., The structure and genesis of limestones at the boundary between the Abalak and Bazhenov formations in Central West Siberia, *Moscow Univ. Geol. Bull.*, 2015, vol. 70, no. 5, pp. 428–435.
- Zakharov, V.A., The formation conditions of the Volgian–Berriasian high-carbon Bazhenov Formation (Western Siberia) according to the paleoecological data, in *Evolutsiya biosfery i bioraznoobraziya* (Evolution of the Biosphere and Biodiversity), Moscow: T-vo Nauchn. Izd. KMK, 2006, pp. 552–568.
- Zanin, Y.N., Luchinina, V.A., Levchuk, M.A., and Pisareva, G.M., Stromatolites and oncolites in Mesozoic deposits of the west Siberian plate, *Russ. Geol. Geophys.*, 2001, vol. 42, pp. 1348–1352.
- Zelenin, N.I. and Ozerov, I.M., *Spravochnik po goryuchim slantsam* (Handbook on Oil Shale), Moscow, 1983.
- Zubkov, M.Yu., Reservoirs in the Bazhenov–Abalak complex of the Western Siberia and methods of forecasting its spread, *Geol. Nefti Gaza*, 2014, no. 5, pp. 58–72.
- Zubkov, M.Yu., Mineral composition and ^{13}C value of fractured carbonate rocks of the Bazhenov–Abalak complex of Western Siberia, *Trudnoizylekaemye Zapasy i Netraditsionnye Istochniki UV*, 2017, no. 6, pp. 67–81.

Translated by M. Hannibal

Publisher's Note. Allerton Press remains neutral with regard to jurisdictional claims in published maps and institutional affiliations.